JOURNAL OF COMPUTATIONAL PHYSICS 20, 220–237 (1976)

Numerical Analysis of Fluid-Hammer Waves by the Method of Characteristics

YONG WOO SHIN AND RICHARD A. VALENTIN

Argonne National Laboratory, Argonne, Illinois 60439

Received February 3, 1975; revised July 21, 1975

The quasi-linear hyperbolic differential equations governing fluid-hammer phenomena in a two-dimensional plane or axisymmetric system are written as integrals along bi-characteristics and a streamline. A stepwise solution procedure is constructed by replacing the integrals by approximation formulas. Derivatives of dependent variables in directions outside the characteristic cone are eliminated and explicit solutions are obtained by linearly combining the remaining difference relations. Two solution schemes resulting from the two approximation formulas are examined for their numerical stability.

Numerical calculations are carried out for a plane acoustic wave diffracting from a 90° sharp corner, and the result is compared with analytical solutions and experiment. Numerical results are further obtained for a simple problem involving a sudden expansion and contraction and the results are compared with one-dimensional acoustic solutions.

INTRODUCTION

Basically, there are two different methods of numerical integration for hyperbolic partial differential equations: (1) The direct finite-difference method, and (2) the method of characteristics. The finite-difference method uses either the artificial viscosity [1] or a special differencing scheme [2]. Both schemes can use rectangular grids and are readily amenable to direct machine coding. Nevertheless, the solution is inherently diffused, and discontinuities or steep gradients in the solution can be unrealistically spread out. This difficulty can be minimized in the method of characteristics since the equations are rendered in a characteristic form before applying the finite-difference approximation such that equations include derivatives only in directions that the solution is extendible. Consequently, this method is potentially more accurate, although it is logically more complex and requires an extensive programming effort.

The method of characteristics, involving more than two independent variables, has been considered since late in the 1940's. Some of the early works include Thornhill [3], Coburn and Dolph [4], Holt [5], and Butler [6], and more recently,

Sauer [7] and Richardson [8]. Many variations exist in the methods used by these investigators. They arise mainly as a result of the inherent weak formulation of the multidimensional method, namely, there exist infinitely many lines along which the equations can be integrated. Coburn and Dolph proposed a method, further developed by Holt, that considers two bicharacteristics and a curve that is the intersection of the two characteristic surfaces through the two chosen bicharacteristics. Sauer used curves called nearcharacteristics that lie outside the characteristic cone. In both of these methods, the solution refers directly to conditions outside the true domain of dependence, and its effect on the numerical results is not well known. Butler and Richardson used four bicharacteristics and a stream line that always fall inside the cone.

In this paper, a three-variable method is discussed that specializes to the particular problem of the propagation of fluid-hammer waves. Two different schemes are considered: One that is essentially the same scheme as discussed in Butler and also in Richardson, and the other a slight variation of it. Both schemes use four bicharacteristics and one streamline, in which the compatibility relations written as integrals are approximated in two different ways. The von Neumann stability test performed for these schemes revealed that a more stringent condition is required on the time step than the Courant–Friedrichs–Lewy (CFL) [9] criterion. Numerical dispersion resulting from the restrictive time step is discussed by a comparison of the numerical results with exact analytical solutions.

Governing Equations

In flows involving large changes in pressure or rapidly varying unsteady motions, the small compressibility of liquids is of primary importance. In short-duration transients, the passive viscous effects are small compared to the more important unsteady and pressure terms.

The basic differential equations describing the fluid-hammer phenomena in a two-dimensional domain are:

Continuity,

$$\frac{\partial \rho}{\partial t} + u\frac{\partial \rho}{\partial r} + w\frac{\partial \rho}{\partial z} + \rho\left(\frac{\partial u}{\partial r} + \nu\frac{u}{r} + \frac{\partial w}{\partial z}\right) = 0; \tag{1}$$

Momentum,

$$\frac{\partial u}{\partial t} + u\frac{\partial u}{\partial r} + w\frac{\partial u}{\partial z} + \frac{1}{\rho}\frac{\partial p}{\partial r} = 0, \tag{2}$$

$$\frac{\partial w}{\partial t} + u\frac{\partial w}{\partial r} + w\frac{\partial w}{\partial z} + \frac{1}{\rho}\frac{\partial p}{\partial z} = 0; \tag{3}$$

Isentropic relation,

$$\left(\frac{\partial p}{\partial \rho}\right)_s = a^2, \tag{4}$$

where $\nu = 0$ for Cartesian and $\nu = 1$ for cylindrical geometry. (This equation replaces the equation of state in a more general problem of a fully compressible flow. The fluid-hammer speed a is assumed to be a constant.) Since the change in density is negligible, and it is difficult to handle this small change, the terms involving the derivatives of density are eliminated by combining Eqs. (1) and (4):

$$\frac{\partial p}{\partial t} + u\frac{\partial p}{\partial r} + w\frac{\partial p}{\partial z} + \rho a^2\left(\frac{\partial u}{\partial r} + \nu\frac{u}{r} + \frac{\partial w}{\partial z}\right) = 0. \tag{5}$$

Equations (2), (3), and (5) do not contain any derivatives of the density and they are conveniently used in the numerical solution, where the density appearing in these equations explicitly is treated as a constant.

Characteristic Formulation

The method of characteristics [10, 11] is used, by an appropriate choice of coordinates, to replace the original system of partial differential equations by a set of compatibility relations involving characteristic coordinates in terms of which the differentiation becomes considerably simplified. The indeterminacy condition of the derivatives of the solution in the direction normal to the characteristic manifold requires the characteristic determinant to vanish, i.e.,

$$\begin{vmatrix} \dfrac{\partial \phi}{\partial t} + u\dfrac{\partial \phi}{\partial r} + w\dfrac{\partial \phi}{\partial z} & 0 & \dfrac{\partial \phi}{\partial r} \\ 0 & \dfrac{\partial \phi}{\partial t} + u\dfrac{\partial \phi}{\partial r} + w\dfrac{\partial \phi}{\partial z} & \dfrac{\partial \phi}{\partial z} \\ a^2\dfrac{\partial \phi}{\partial r} & a^2\dfrac{\partial \phi}{\partial z} & \dfrac{\partial \phi}{\partial t} + u\dfrac{\partial \phi}{\partial r} + w\dfrac{\partial \phi}{\partial z} \end{vmatrix} = 0, \tag{6}$$

where ϕ is the characteristic coordinate normal to the characteristic manifold. If $\boldsymbol{\lambda}$ is a vector parallel to the ϕ-coordinate, its components λ_0, λ_1, and λ_2 in the direction of the t, r, and z coordinate are $\partial\phi/\partial t$, $\partial\phi/\partial r$, and $\partial\phi/\partial z$, respectively. Equation (6) yields a third-order polynomial that determines $\boldsymbol{\lambda}$:

$$\left(\frac{\partial \phi}{\partial t} + u\frac{\partial \phi}{\partial r} + w\frac{\partial \phi}{\partial z}\right)\left[\frac{\partial \phi}{\partial t} + u\frac{\partial \phi}{\partial r} + w\frac{\partial \phi}{\partial z} + a\left(\left(\frac{\partial \phi}{\partial r}\right)^2 + \left(\frac{\partial \phi}{\partial z}\right)^2\right)^{1/2}\right]$$
$$\times\left[\frac{\partial \phi}{\partial t} + u\frac{\partial \phi}{\partial r} + w\frac{\partial \phi}{\partial z} - a\left(\left(\frac{\partial \phi}{\partial r}\right)^2 + \left(\frac{\partial \phi}{\partial z}\right)^2\right)^{1/2}\right] = 0. \tag{7}$$

Bicharacteristics

The characteristic equations (three equations resulting from Eq. (7)) are of the Hamilton–Jacobi type of which solutions are the canonical equations that are also called bicharacteristics:

$$\frac{dr}{dt} = u, \tag{8a}$$

$$\frac{dz}{dt} = w; \tag{8b}$$

$$\frac{dr}{dt} = u \pm a \frac{\partial\phi/\partial r}{((\partial\phi/\partial r)^2 + (\partial\phi/\partial z)^2)^{1/2}}, \tag{9a}$$

$$\frac{dz}{dt} = w \pm a \frac{\partial\phi/\partial z}{((\partial\phi/\partial r)^2 + (\partial\phi/\partial z)^2)^{1/2}}. \tag{9b}$$

Notice that Eqs. (8) define the streamline, whereas Eqs. (9) represent a multitude of bicharacteristics lying on the surface of the two generalized cones that are the envelopes of all the characteristic manifolds at any point. The + and − signs in Eqs. (9) refer to the bicharacteristics on the upper and lower cone, respectively. Figure 1 depicts the geometric description of the generalized cone, streamline,

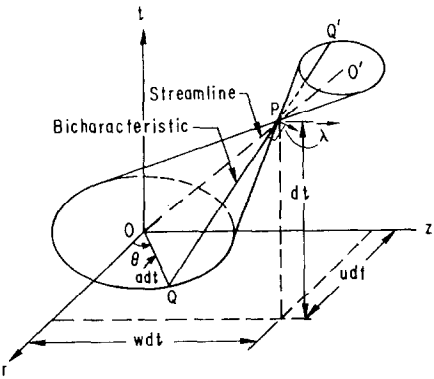

FIG. 1. Streamline, bicharacteristic, and characteristic cone at P in t–r–z space.

and bicharacteristics, where the vector $\boldsymbol{\lambda}$ indicated in the figure is a particular $\boldsymbol{\lambda}$ that is normal to a particular manifold intercepting the cones along the bicharacteristic $\overline{QPQ'}$. Only the lower cone is considered, in which the base circle (the circle with center O in Fig. 1) is placed in the initial surface while the general point P

is located at a point a small increment dt advanced in time. It can be shown that a bicharacteristic on the lower cone can be expressed parametrically as

$$\begin{aligned} dr &= (u - a\cos\theta)\,dt, \\ dz &= (w - a\sin\theta)\,dt, \end{aligned} \tag{10}$$

where the angle θ is measured counterclockwise as time increases (see Fig. 1).

Compatibility Relations

Equations (2), (3), and (5), the original system of partial differential equations, are linearly combined to yield compatibility relations that involve differentiation along bicharacteristics:

$$\cos\theta\frac{du}{dt} + \sin\theta\frac{dw}{dt} - \frac{1}{\rho a}\frac{dp}{dt} - a \times \left[\sin^2\theta\frac{du}{dr} - \sin\theta\cos\theta\left(\frac{\partial u}{\partial z} + \frac{\partial w}{\partial r}\right) + \cos^2\theta\frac{dw}{dz} + \nu\frac{u}{r}\right] = 0, \tag{11}$$

where d/dt represents the differentiation along a bicharacteristic. Along the streamline, Eq. (5) is used. As will be discussed later, the choice of angle θ, 0, $\pi/2$, π, and $3\pi/2$, considerably simplifies the equations, and the resulting four equations together with the one along the streamline are sufficient to solve for the five unknowns u, w, p, $\partial u/\partial r$, and $\partial w/\partial z$ appearing in the equations. In actual calculations, the five equations are linearly combined to eliminate the two derivatives and the remaining three equations are finally used to solve for the desired three flow variables.

Numerical Procedure

The compatibility relations are written first as integrals along the four bicharacteristics and the streamline. The compatibility relations

$$\begin{aligned} &\int \cos\theta_n\,du + \int \sin\theta_n\,dw - \frac{1}{\rho a}\int dp \\ &\quad = a\int\left[\sin^2\theta_n\frac{\partial u}{\partial r} - \sin\theta_n\cos\theta_n\left(\frac{\partial u}{\partial z} + \frac{\partial w}{\partial r}\right) + \cos^2\theta_n\frac{\partial w}{\partial z} + \nu\frac{u}{r}\right]dt, \end{aligned} \tag{12}$$

hold along the four bicharacteristics ($n = 1, 2, 3$, and 4), defined by

$$\int dr = \int (u - a\cos\theta_n)\,dt, \tag{13a}$$

$$\int dz = \int (w - a\sin\theta_n)\,dt, \tag{13b}$$

and the relation

$$\int dp = -\rho a^2 \int \left(\frac{\partial u}{\partial r} + \frac{\partial w}{\partial z} + \nu \frac{u}{r}\right) dt \tag{14}$$

applies along the streamline, defined by

$$\int dr = \int u\, dt, \tag{15a}$$

$$\int dz = \int w\, dt. \tag{15b}$$

In Eqs. (12) and (13), the angles θ_n will, in general, vary along the bicharacteristics. This was discussed by both Butler [6] and Richardson [8].

A procedure similar to Richardson's is employed to obtain an expression for the change in the angle θ:

$$\Delta\theta = -\left(-\sin\alpha\cos\alpha\frac{\partial u}{\partial r} + \cos^2\alpha\frac{\partial u}{\partial z} - \sin^2\alpha\frac{\partial w}{\partial r} + \sin\alpha\cos\alpha\frac{\partial w}{\partial z}\right) dt + O(\Delta t)^2. \tag{16}$$

Here, α denotes the angle at the cone vertex, $\Delta\theta = \theta - \alpha$, where θ is the angle away from the cone vertex, and the spatial derivatives are to be evaluated in the initial time plane (see Fig. 2 for the finite-difference network used in the numerical procedure). A brief derivation of Eq. (16) is given in the Appendix.

Two different numerical schemes are considered here; one that is basically the same as the one discussed in Butler or Richardson in which the integrals are approximated by a trapezoidal formula and the other employing a lower-order approximation in which the integrands are evaluated at the cone vertex P. Thus, the former scheme yields the second-order accurate solution while the latter is

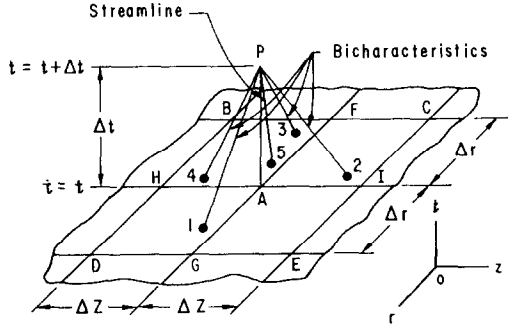

FIG. 2. Streamline and bicharacteristics in finite-difference grids.

essentially a first-order solution scheme. (Because of the assumptions associated with Eqs. (29), it is not clear whether the former scheme is truly a second-order scheme. In the linear limit, it can be shown that the bicharacteristic angle θ remains unchanged and hence, the scheme is a second-order accurate method involving an error of $O(\Delta t^2)$. In any event, the distinction of second- and first-order scheme will be used throughout this paper for convenience.)

A considerable simplification is realized in the first-order approximation since Eq. (16) is no longer needed. Computational efficiency is also enhanced since the numerical procedure requires no spatial derivatives to be evaluated numerically.

In both schemes, the choice of $\alpha = 0, \pi/2, \pi$, and $3\pi/2$ eliminates the derivatives $\partial u/\partial z$ and $\partial w/\partial r$ from the discretized system of five equations (five compatibility relations along four bicharacteristics and one streamline) and the two remaining derivatives $\partial u/\partial r$ and $\partial w/\partial z$ are further eliminated by a linear combination of the five equations. The resulting three equations are then used to obtain an explicit expression for the desired flow variables u, w, and p. The nonlinear characteristic equations require an iterative numerical procedure. Due to the directional integration procedure, the values of variables u, w, p, $\partial u/\partial r$, and $\partial w/\partial z$ are required at points at which the bicharacteristics and the streamline intersect the current time-plane. These points, in general, fall between the gridpoints. The characteristic relations, Eqs. (13) and (15), are used in locating these intersections. In the second-order method, Eq. (16) also has to be used simultaneously in locating the intercepts as well as in evaluating the integrands of Eq. (12). Once the intercepts are located, the values of the dependent variables at these points are calculated using the four-point bivariate formula. Figure 2 depicts the finite-difference network employed in the numerical procedure that uses fixed grid spacings and time step. Points 1–5 shown in this figure are the intercepts of the four bicharacteristics and one streamline all passing through point P with the current time-plane. The values of u and $\partial u/\partial r$ at point 2, for example, are determined as follows:

$$u_2 = \left(1 - \frac{\Delta r_2}{\Delta r}\right)\left(1 - \frac{\Delta z_2}{\Delta z}\right) u_A + \frac{\Delta r_2}{\Delta r}\left(1 - \frac{\Delta z_2}{\Delta z}\right) u_F + \left(1 - \frac{\Delta r_2}{\Delta r}\right)\frac{\Delta z_2}{\Delta z}\, u_I + \frac{\Delta r_2}{\Delta r}\frac{\Delta z_2}{\Delta z}\, u_C ,$$

$$\left(\frac{\partial u}{\partial r}\right)_2 = \left(1 - \frac{\Delta z_2}{\Delta z}\right)\frac{u_G - u_F}{2\,\Delta r} + \frac{\Delta z_2}{\Delta z}\,\frac{u_E - u_C}{2\,\Delta r} .$$

It is to be noted that the expression for the derivatives approaches a central difference in the linear limit, i.e., $(u, w) \ll a$.

For each unknown point, namely, point P of Fig. 2, the coordinates $r_1, r_2, \ldots, r_5, z_1, z_2, \ldots,$ and z_5 of the intercepts are first estimated by approximating the integrands of the characteristic equations by their values taken at the gridpoint

A (see Fig. 2). $\Delta\theta_n = 0$ is also assumed so that $\theta_n = \alpha_n = \text{const}$. The values of flow variables u, w, p and the derivatives $\partial u/\partial r$ and $\partial w/\partial z$ at these points are next calculated using the bivariate formula and linear interpolation as discussed above. Finally, the values of u, w, and p at point P are solved using the three relations. This procedure for an unknown point P is repeated until a satisfactory convergence is attained, where in each iteration the most current solution is used in evaluating the integrals of the characteristic equations and compatibility relations. The advancement of the solution by one time-step requires this iterative procedure for all gridpoints lying in the advanced time-plane.

At the boundary (or the axial-point in the case of cylindrical geometry), not all five equations are available since some bicharacteristic may fall outside the computational domain. The procedure for these points is essentially the same except that the missing equations must supplemented by appropriate boundary or axial-point conditions.

Boundary and Axial-Point Conditions

The boundary conditions considered here are those that are consistent with the inviscid flows. Walls are treated as rigid on which the normal component of the velocity vector vanishes, while the tangential component is left free. At the axis of symmetry, in the case of cylindrical geometry, i.e., $r = 0$, the radial component is set to zero and the term u/r is replaced by $\partial u/\partial r$.

Numerical Stability

The CFL [9] criterion provides the necessary condition for stability and convergence of approximate finite-difference relations in hyperbolic systems. With reference to Fig. 2, the condition requires that the bicharacteristics and the streamline through P all fall inside the rectangle $BCED$. Thus, the domain of dependence of the difference system contains the domain of dependence of the differential system.

The von Neumann test [12] is performed here to obtain more specific conditions for stability of the two schemes discussed in this paper. It is prohibitively difficult to treat these schemes in their complete forms; hence, only simplified versions are considered and the end results are justified by numerical experimentation. The second-order scheme is first simplified by assuming $\Delta\theta_n = 0$. (Under this assumption, the scheme is no longer a true second-order scheme. Nevertheless, it will be called the second-order solution scheme, mainly for convenience.) An explicit expression of this scheme is obtained by a linear combination of the three reduced equations as described earlier:

$$u = \tfrac{1}{2}[u_1 - u_3 - (1/\rho a)(p_1 - p_3) + \tfrac{1}{2}a\,\Delta t(b_1 - b_3)], \tag{17a}$$

$$w = \tfrac{1}{2}[w_2 + w_4 - (1/\rho a)(p_2 - p_4) + \tfrac{1}{2}a\,\Delta t(b_2 - b_4)], \tag{17b}$$

$$p = (\rho a/2)[-u_1 + u_3 - w_2 + w_4 + (1/\rho a)(p_1 + p_2 + p_3 + p_4 - 2p_5) - \tfrac{1}{2}a\,\Delta t(b_1 + b_2 + b_3 + b_4 - 2b_5 + 2\nu(u/r))], \tag{17c}$$

where

$$b_n = (\sin^2\alpha(\partial u/\partial r) + \cos^2\alpha(\partial w/\partial z) + \nu(u/r))_n\,, \tag{17d}$$

$n = 1, 2, 3$, or 4 depending on whether α is $0, \pi/2, \pi$, or $3\pi/2$, and

$$b_5 = ((\partial u/\partial r) + (\partial w/\partial z) + \nu(u/r))_5\,. \tag{17e}$$

For further simplification, the characteristic equations are linearized under the acoustic approximation ($u, w \ll a$):

$$\Delta z_1 = |\, z_p - z_1\,| \cong 0, \tag{18a}$$

$$\Delta z_3 = |\, z_p - z_3\,| \cong 0, \tag{18b}$$

$$\Delta r_2 = |\, r_p - r_2\,| \cong 0, \tag{18c}$$

$$\Delta r_4 = |\, r_p - r_4\,| \cong 0. \tag{18d}$$

The analysis given in the following is restricted to the plane two-dimensional case ($\nu = 0$). The axisymmetric case can be treated essentially in the same manner and it is found that the results obtained here for the plane case apply equally well to the axisymmetric case. The dependent variables are written as a double Fourier series and its each component is examined as to its growth with time. A Fourier component of the dependent variable u, for example, at any gridpoint ($j\,\Delta r, k\,\Delta z$) and at any time-level $n\,\Delta t$ is written as

$$u(j\,\Delta r, k\,\Delta z, n\,\Delta t) = u_0{}^n e^{i\alpha j\Delta r} e^{i\beta k\Delta z}, \tag{19a}$$

and the same quantity at an advanced time-level $(n + 1)\,\Delta t$ as

$$u(j\,\Delta r, k\,\Delta z, (n + 1)\,\Delta t) = u_0^{n+1} e^{i\alpha j\Delta r} e^{i\beta k\Delta z}, \tag{19b}$$

where α and β are the wave numbers associated with the r- and z-coordinate, and $u_0{}^n$ and u_0^{n+1} are the time factors at the current and advanced time-level, respectively. Similar expressions can be written for the other two variables. The substitution of these expressions in the solution scheme (17) and simplification yield a linear system of the time factors of the form

$$\begin{pmatrix} u_0^{n+1} \\ w_0^{n+1} \\ p_0^{n+1} \end{pmatrix} = A(\alpha\,\Delta r, \beta\,\Delta z, \Delta t) \begin{pmatrix} u_0{}^n \\ w_0{}^n \\ p_0{}^n \end{pmatrix}, \tag{20}$$

where A is the amplification matrix. The requirement for numerical stability is that the spectral radius of the amplification matrix (i.e., the maximum of the

absolute value of the eigenvalues) be less than unity [13]. Since the characteristic relations are linearized, only simple linear interpolations are required (in obtaining the matrix A) in the evaluation of the values of the dependent variables (u_1, u_2,..., etc.) and the derivatives ($\partial u/\partial r$ and $\partial w/\partial z$) in the current time-plane. For example, $u_1 = (\Delta r_1/\Delta r)\,u_G + (1 - (\Delta r_1/\Delta r))\,u_A$,..., $(\partial w/\partial z)_2 = (\Delta r_1/\Delta r) \times (w_E - w_D)/2\,\Delta z + (1 - \Delta r_1/\Delta r)(w_I - w_H)/2\,\Delta z$,..., etc., where the subscripts refer to the specific gridpoints in the current time-plane as shown in Fig. 2.

Since the same condition was found for stability of both of the two schemes and, moreover, the procedure is also essentially the same, the analysis here is restricted to the simpler first-order scheme. The first-order solution scheme is obtained by evaluating the integrands as their values at the unknown point, thus, eliminating the spatial derivatives (which appear in the second-order scheme) to be evaluated in the current time-plane:

$$u = \tfrac{1}{2}[u_1 + u_3 + (1/\rho a)(-p_1 + p_3)], \tag{21a}$$

$$w = \tfrac{1}{2}[w_2 + w_4 + (1/\rho a)(-p_2 + p_4)]; \tag{21b}$$

$$p = \tfrac{1}{2}\rho a[-u_1 + u_3 - w_2 + w_4 + (1/\rho a)(p_1 + p_2 + p_3 + p_4 - 2p_5)]. \tag{21c}$$

Thus, the amplification matrix obtained for this scheme is:

$$A = \frac{1}{2}\begin{bmatrix} 2+ & & (1 - e^{i\alpha\Delta r})\dfrac{\Delta r_1}{\Delta r} \\ (-1 + e^{i\alpha\Delta r})\dfrac{\Delta r_1}{\Delta r} & 0 & +(-1 + e^{-i\alpha\Delta r})\dfrac{\Delta r_3}{\Delta r} \\ +(-1 + e^{-i\alpha\Delta r})\dfrac{\Delta r_3}{\Delta r} & & \end{bmatrix}$$

$$\begin{bmatrix} & 2+ & \\ 0 & (-1 + e^{i\beta\Delta z})\dfrac{\Delta z_2}{\Delta z} & (1 - e^{i\beta\Delta z})\dfrac{\Delta z_2}{\Delta z} \\ & +(-1 + e^{-i\beta\Delta z})\dfrac{\Delta z_4}{\Delta z} & +(-1 + e^{-i\beta\Delta z})\dfrac{\Delta z_4}{\Delta z} \end{bmatrix}$$

$$\begin{bmatrix} & & 2+ \\ (1 - e^{i\alpha\Delta r})\dfrac{\Delta r_1}{\Delta r} & (1 - e^{i\beta\Delta z})\dfrac{\Delta z_2}{\Delta z} & (-1 + e^{i\alpha\Delta r})\dfrac{\Delta r_1}{\Delta r} \\ +(-1 + e^{-i\alpha\Delta r})\dfrac{\Delta r_3}{\Delta r} & +(-1 + e^{-i\beta\Delta z})\dfrac{\Delta z_4}{\Delta z} & +(-1 + e^{i\beta\Delta z})\dfrac{\Delta z_2}{\Delta z} \\ & & +(-1 + e^{-i\alpha\Delta r})\dfrac{\Delta r_3}{\Delta r} \\ & & +(-1 + e^{-i\beta\Delta z})\dfrac{\Delta z_4}{\Delta z} \end{bmatrix}. \tag{22}$$

Although it is very difficult to obtain the eigenvalues of this matrix in its general form, the consideration of various particular choices for the values of $\alpha\,\Delta r$ and $\beta\,\Delta z$ revealed that the matrix possesses the greatest eigenvalues in the absolute value when both $e^{\pm i\alpha\Delta r}$ and $e^{\pm i\beta\Delta z}$ take on the value -1. For this choice, the eigenvalues (γ) are determined by the polynomial,

$$\left(1-\frac{\Delta r_1}{\Delta r}-\frac{\Delta r_3}{\Delta r}-\gamma\right)\left(1-\frac{\Delta z_2}{\Delta z}-\frac{\Delta z_4}{\Delta z}-\gamma\right)\left(1-\frac{\Delta r_1}{\Delta r}-\frac{\Delta r_3}{\Delta r}-\frac{\Delta z_2}{\Delta z}-\frac{\Delta z_4}{\Delta z}-\gamma\right)=0, \tag{23}$$

from which the stability of the first-order scheme, Eqs. (22), is determined as follows:

$$\frac{\Delta r_1}{\Delta r}+\frac{\Delta r_3}{\Delta r}+\frac{\Delta z_2}{\Delta z}+\frac{\Delta z_4}{\Delta z}\leqslant 2. \tag{24}$$

In the linear limit, i.e., $\Delta r_1=\Delta r_3$ and $\Delta z_2=\Delta z_4$, and if $\Delta r=\Delta z$ also, it is seen that Eq. (24) reduces to

$$a\,\Delta t\leqslant \tfrac{1}{2}\,\Delta z,$$

which indicates that the time step required for stability of the scheme under consideration is approximately only one-half of the one required by the CFL criterion. As will be seen later, this result of the von Neumann test is in agreement with the results of numerical experiments.

Analytical Solutions

To verify the numerical schemes, analytical solutions are considered for comparison with numerical results for simple acoustic problems of plane pressure discontinuities diffracting from a 90° sharp corner. The technique used is Busemann's [14] conical flow method by which the two-dimensional wave equation (plane case, $\nu=0$) is transformed into the Laplace equation. The potential problem is then solved by a conformal mapping to a unit circle. Keller and Blank [15] carried out the procedure and obtained a closed form solution for a plane wave diffracting from a wedge of an arbitrary angle. Following the solution procedure as outlined in Keller and Blank, analytical solutions are obtained for plane discontinuities compressing and expanding around a 90° sharp corner. The results are plotted in Figs. 3–5. Also plotted for comparison in the figures are the numerical results obtained using the linearized acoustic equations and the experiment of White and Bleakney [16] for the case of compressing waves. (For this case of compressing waves, the analytical solution given in Fig. 4 is identical to the one given in Keller [17].) A good agreement is shown between the three results in general except near the corner and the discontinuity front. The deviation of the

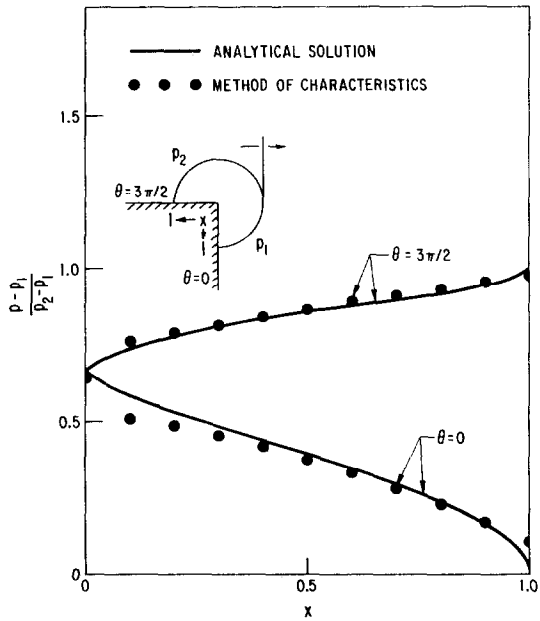

FIG. 3. Expansion of plane pressure discontinuity around 90° sharp corner.

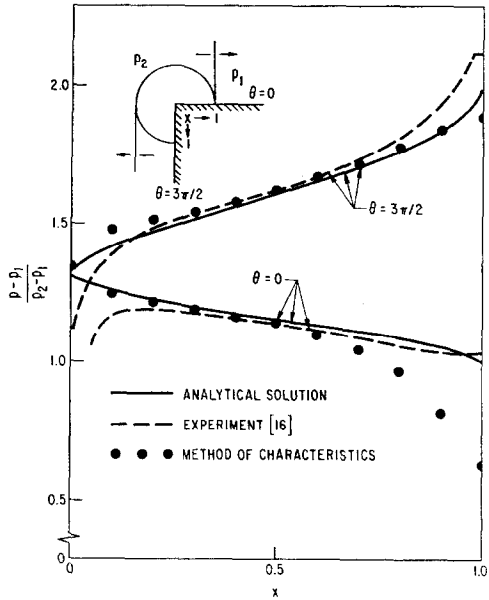

FIG. 4. Compression of plane pressure discontinuity around 90° sharp corner.

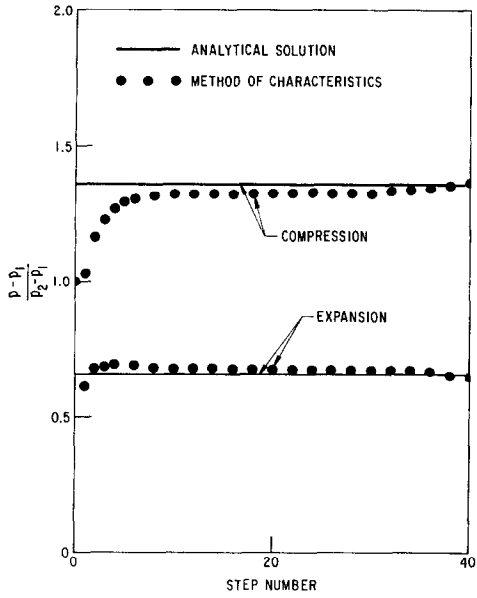

FIG. 5. Pressure-time history at 90° sharp corner.

experiment from the analytical and the numerical solution near the corner, as shown in Fig. 4, is attributed to the viscous vortex effects, which are neglected in the analytical and numerical procedure. The discrepancy shown between the numerical result and the analytical solution (also the experiment near the discontinuity front $\theta = 0$, $x \approx 1$ in Fig. 4) is mainly due to the numerical dispersion resulting from the restrictive time steps required for numerical stability, as discussed earlier.

The time history of the pressure at the corner is given in Fig. 5 for both cases of the expansion and compression. A good agreement is again shown between the analytical solution and the numerical results.

SAMPLE PROBLEM

A simple problem involving a sudden expansion and contraction in an axisymmetric geometry is calculated. The numerical results confirmed the findings of the von Neumann stability test performed for the two numerical schemes considered in this paper. Figure 6 depicts the problem configuration. A step pressure-pulse Δp of 1000 psi is used as the source of distrubance located far upstream in the system, which is assumed to be filled with stationary water at 50 psi.

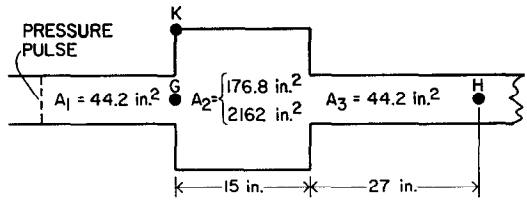

FIG. 6. Sample problem.

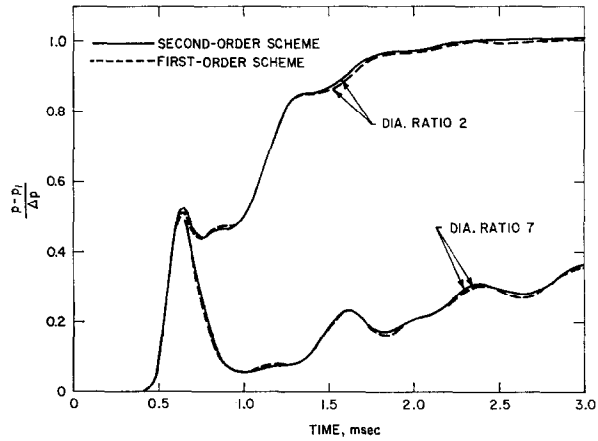

FIG. 7. Comparison of pressure at point G obtained by first- and second-order schemes.

For the one-dimensional distrubance considered here, the flow in regions far from the expansion and contraction will be planar. Hence, the computational domain is divided into two separate regions. The one-dimensional domain consists of the regions away from the transitions, whereas the central region including the expansion and contraction is considered two-dimensional.

In the one-dimensional domain, the three variable formulation discussed in this paper reduces to the more-familiar two-variable method. Only two compatibility relations corresponding to the bicharacteristic angles $\pi/2$ and $3\pi/2$ need to be considered. At the boundaries that divide the two regions, simplified conditions $u = \partial u/\partial r = \partial w/\partial r = 0$ are used. In the numerical calculation, square grids with constant density are employed using five nodes across the radius of the small diameter pipes. The time step is chosen to meet the von Neumann condition, Eq. (24).

Figure 7 shows a typical comparison of the two calculations obtained by the two numerical schemes considered, in which the pressure at point G of Fig. 6 is plotted against time. It is seen that the first- and second-order methods yielded nearly identical results. Figure 8 and 9 depict the pressures at point G and H respectively. Also plotted in these figures are the one-dimensional acoustic solution

[18] and the numerical solution based on one-dimensional treatment for the entire region. As suspected, a close agreement is seen between the acoustic solution and the one-dimensional numerical result. The dispersion effects resulting from the restrictive time steps of the two-dimensional formulation are exemplified by the smeared wave front that is more pronounced in the two-dimensional result than the one-dimensional solution as shown in Fig. 9. In general, the two-dimensional calculation followed the one-dimensional solution. As can be seen in Fig. 8,

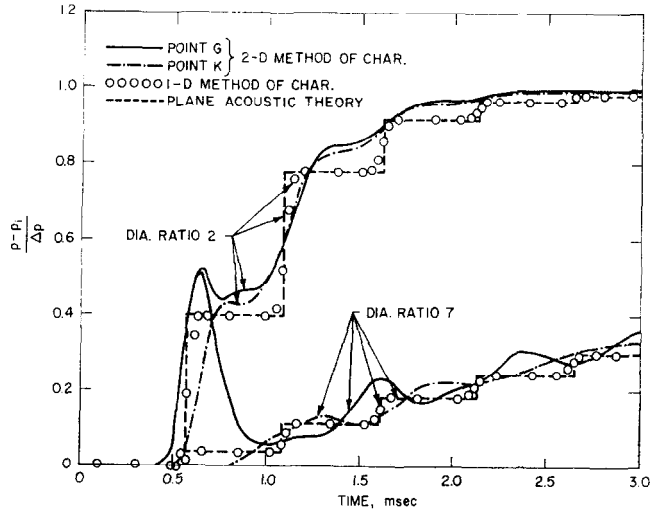

FIG. 8. Pressure vs time at the expansion points (points G and K).

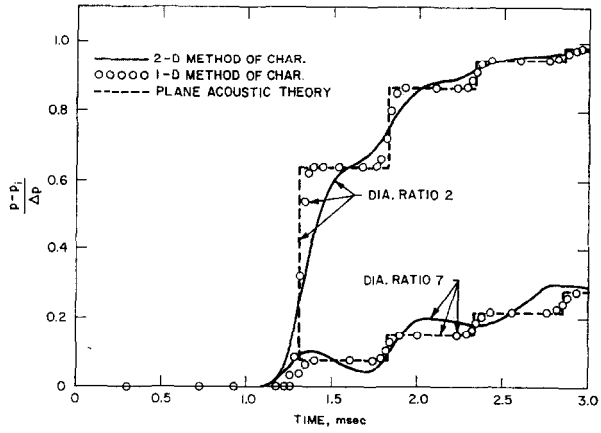

FIG. 9. Pressure vs time at point H.

the most disagreement is indicated in the case of large diameter ratio (diameter ratio 7) since a significant two-dimensionality prevails near point G (see Fig. 6) during passage of the wavefront. This is evidenced by the large difference in the pressures between points G and K (in the case of diameter ratio 7) for the time duration 0.5 to 1.0 msec. Near one-dimensionality is shown at point H even for the diameter ratio 7, exhibiting a good agreement between the one- and two-dimensional calculation (see Fig. 9).

Conclusions

This paper discusses the numerical analysis of multidimensional fluid-hammer phenomena using the method of characteristics. Specifically, an explicit solution procedure is constructed along bicharacteristics and streamline such that no direct reference is made to conditions outside the true domain of dependence. Two numerical schemes evolving from two different approximations of the integral relations yielded essentially identical numerical results. The von Neumann stability test performed for these schemes revealed that a more restrictive condition is required on the time step than the necessary CFL criterion. Sample calculations and their comparison with analytical results indicate that significant errors may arise in the neighborhood of steep discontinuity fronts as results of the inherent numerical dispersion. Nevertheless, the accuracy and efficiency of the basic method have been demonstrated. The first-order scheme in particular has proved useful, especially for handling irregular boundaries, since the scheme requires no spatial derivatives to be evaluated numerically. The method used in the sample problem is well suited to cases where only limited regions of a complex network require two-dimensional treatment. For such problems, it provides the needed resolution in the region of primary interest and, by collapsing the procedure into the conventional two-variable formulation, allows the remaining region to be computed in a one-dimensional manner.

Appendix

Let the equations describing the surface of a characteristic cone be

$$r = r(\alpha, \tau), \qquad z = z(\alpha, \tau), \qquad t = t(\alpha, \tau),$$

where $\tau = -t$ and α is the bicharacteristic angle at the cone vertex. The bicharacteristic equations are

$$\frac{\partial r}{\partial \tau}(\alpha, \tau) = -u + a \cos \theta, \tag{25a}$$

$$\frac{\partial z}{\partial \tau}(\alpha, \tau) = -w + a \sin \theta, \tag{25b}$$

where θ is the bicharacteristic angle away from the cone vertex. If u, w, and θ are assumed to be locally constants, the following approximate relationship holds:

$$\cos\theta(\partial r/\partial\alpha)(\alpha,\tau) = -\sin\theta(\partial z/\partial\alpha)(\alpha,\tau), \tag{26}$$

which approaches an exact relationship as $\theta \to \alpha$ or $\tau \to 0$.

Consider a bicharacteristic with angle α at P (refer to Fig. 1) and let τ increase. An expression for the angle θ is sought here as a function of τ. Assume that the unknowns along a bicharacteristic are linear in τ and the coefficients depend only on α, i.e.,

$$u = u_0 + [u(\alpha) - u_0]\,\tau, \tag{27a}$$

$$w = w_0 + [w(\alpha) - w_0]\,\tau, \tag{27b}$$

$$\theta = \alpha + [\theta(\alpha) - \alpha]\,\tau, \tag{27c}$$

where u_0, w_0 are the values of u and w at P. Substituting Eqs. (27) into Eqs. (25) and integrating yields

$$r(\alpha,\tau) = r_0 + (-u_0 + a\cos\alpha)\,\tau + \tfrac{1}{2}\{-u(\alpha) + u_0 - \sin\alpha[\theta(\alpha) - \alpha]\}\,\tau^2 + O(\tau^3), \tag{28a}$$

$$z(\alpha,\tau) = z_0 + (-w_2 + a\sin\alpha)\,\tau + \tfrac{1}{2}\{-w(\alpha) + w_0 + a\cos\alpha[\theta(\alpha) - \alpha]\}\tau^2 + O(\tau^3), \tag{28b}$$

where r_0 and z_0 are r and z coordinates, respectively, of the cone apex. Hence,

$$\frac{\partial r}{\partial\alpha}(\alpha,\tau) = -a\sin\alpha\tau + \tfrac{1}{2}[-u'(\alpha) + a\sin\alpha - a\theta(\alpha)\cos\alpha + a\alpha\cos\alpha - a\theta'(\alpha)\sin\alpha]\,\tau^2 + O(\tau^3), \tag{29a}$$

$$\frac{\partial z}{\partial\alpha}(\alpha,\tau) = a\cos\alpha\tau + \tfrac{1}{2}[-w'(\alpha) - a\cos\alpha + a\theta'(\alpha)\cos\alpha - a\theta(\alpha)\sin\alpha + a\alpha\sin\alpha]\,\tau^2 + O(\tau^3). \tag{29b}$$

Equations (29) are substituted into Eq. (26) and the leading terms on both sides are equated to yield

$$\theta = \alpha + \left[\cos^2\alpha\frac{\partial u}{\partial z} - \sin^2\alpha\frac{\partial w}{\partial r} + \sin\alpha\cos\alpha\left(-\frac{\partial u}{\partial r} + \frac{\partial w}{\partial z}\right)\right]\tau + O(\tau^2). \tag{30}$$

In Eq. (34), the partial derivatives are to be evaluated in the time-plane $\tau = \tau$.

ACKNOWLEDGMENTS

This work was supported by the Engineering and Components Development Branch, Division of Reactor Research and Development, United States Atomic Energy Commission.

REFERENCES

1. J. VON NEUMANN AND R. D. RICHTMYER, *J. Appl. Phys.* **21** (1950), 232.
2. L. FOX, "Numerical Solution of Ordinary and Partial Differential Equations," p. 218, Addison–Wesley, Reading, Mass., 1962.
3. C. K. THORNHILL, The Numerical Method of Characteristics for Hyperbolic Problems in Three Independent Variables, ARC-RM-2615 (1948).
4. N. COBURN AND C. L. DOLPH, The Method of Characteristics in the Three-dimensional Stationary Supersonic Flow of a Compressible Gas, in "Proceedings of the First Symposium on Applied Mathematics of the American Mathematical Society," p. 55, American Mathematical Society, Providence, R.I., 1949.
5. M. HOLT, *J. Fluid Mech.* **1** (1956), 409.
6. D. S. BUTLER, *Proc. Roy. Soc. London. Ser. A* **255** (1960), 232.
7. R. SAUER, *Numer. Math.* **5** (1963), 55.
8. D. J. RICHARDSON, Solutions of Two-dimensional Hydrodynamic Equations by the Method of Characteristics, in "Methods in Computational Physics" (B. Alder, S. Fernbach, and M. Rotenberg, Eds.), p. 295, Academic Press, New York, 1964.
9. R. COURANT, K. FRIEDRICHS, AND H. LEWY, *Math. Ann.* **100** (1928), 32.
10. A. JEFFREY AND T. TANIUTI, "Nonlinear Wave Propagation," Vol. 9, Academic Press, New York/London, 1964.
11. R. COURANT AND D. HILBERT, "Methods of Mathematical Physics," Vol. 2, Interscience, New York, 1962.
12. G. G. O'BRIEN, M. A. HYMAN, AND S. KAPLAN, *J. Math. and Phys.* **29** (1950), 223.
13. P. FOX, The Solution of Hyperbolic Partial Differential Equations by Difference Methods, in "Mathematical Methods for Digital Computers" (A. Ralston and H. S. Wilf, Eds), Chap. 16, p. 180, Wiley, New York/London, 1960.
14. A. BUSEMANN, Infinitesimal conical supersonic flow, *Schriften Deutschen Akad. Luftfahrforschung* **7B** (1953), 105.
15. J. B. KELLER AND A. BLANK, *Comm. Pure Appl. Math.* **4** (1951), 75.
16. D. R. WHITE AND W. BLEAKNEY, "Shock Loading of Rectangular Structure," Technical Report II-11, Dept. of Physics, Princeton University, 1952.
17. J. KELLER, *J. Appl. Phys.* **23** (1952), 1267.
18. L. E. KINSLER AND A. R. FREY, "Fundamentals of Acoustics," 2nd. ed., Wiley, New York, 1962.